Cellular/Molecular

Synaptotagmins 1 and 7 Play Complementary Roles in Somatodendritic Dopamine Release

Takuya Hikima,[1] Paul Witkovsky,[1] Latika Khatri,[2] Moses V. Chao,[2,3,4] and Margaret E. Rice[1,4]

[1]Department of Neurosurgery, New York University Grossman School of Medicine, New York, New York 10016, [2]Department of Cell Biology, New York University Grossman School of Medicine, New York, New York 10016, [3]Department of Psychiatry, New York University Grossman School of Medicine, New York, New York 10016, and [4]Department of Neuroscience & Physiology, New York University Grossman School of Medicine, New York, New York 10016

The molecular mechanisms underlying somatodendritic dopamine (DA) release remain unresolved, despite the passing of decades since its discovery. Our previous work showed robust release of somatodendritic DA in submillimolar extracellular Ca^{2+} concentration ($[Ca^{2+}]_o$). Here we tested the hypothesis that the high-affinity Ca^{2+} sensor synaptotagmin 7 (Syt7), is a key determinant of somatodendritic DA release and its Ca^{2+} dependence. Somatodendritic DA release from SNc DA neurons was assessed using whole-cell recording in midbrain slices from male and female mice to monitor evoked DA-dependent D2 receptor-mediated inhibitory currents (D2ICs). Single-cell application of an antibody to Syt7 (Syt7 Ab) decreased pulse train-evoked D2ICs, revealing a functional role for Syt7. The assessment of the Ca^{2+} dependence of pulse train-evoked D2ICs confirmed robust DA release in submillimolar $[Ca^{2+}]_o$ in wild-type (WT) neurons, but loss of this sensitivity with intracellular Syt7 Ab or in Syt7 knock-out (KO) mice. In millimolar $[Ca^{2+}]_o$, pulse train-evoked D2ICs in Syt7 KOs showed a greater reduction in decreased $[Ca^{2+}]_o$ than seen in WT mice; the effect on single pulse-evoked DA release, however, did not differ between genotypes. Single-cell application of a Syt1 Ab had no effect on train-evoked D2ICs in WT SNc DA neurons, but did cause a decrease in D2IC amplitude in Syt7 KOs, indicating a functional substitution of Syt1 for Syt7. In addition, Syt1 Ab decreased single pulse-evoked D2ICs in WT cells, indicating the involvement of Syt1 in tonic DA release. Thus, Syt7 and Syt1 play complementary roles in somatodendritic DA release from SNc DA neurons.

Key words: **autoreceptors; D2 dopamine receptors; exocytosis; GIRK channels; substantia nigra; synaptotagmin 1**

Significance Statement

The respective Ca^{2+} dependence of somatodendritic and axonal dopamine (DA) release differs, resulting in the persistence of somatodendritic DA release in submillimolar Ca^{2+} concentrations too low to support axonal release. We demonstrate that synaptotagmin7 (Syt7), a high-affinity Ca^{2+} sensor, underlies phasic somatodendritic DA release and its Ca^{2+} sensitivity in the substantia nigra pars compacta. In contrast, we found that synaptotagmin 1 (Syt1), the Ca^{2+} sensor underlying axonal DA release, plays a role in tonic, but not phasic, somatodendritic DA release in wild-type mice. However, Syt1 can facilitate phasic DA release after Syt7 deletion. Thus, we show that both Syt1 and Syt7 act as Ca^{2+} sensors subserving different aspects of somatodendritic DA release processes.

Introduction

Midbrain dopamine (DA) neurons release DA from their somata and dendrites in the substantia nigra pars compacta (SNc) and ventral tegmental area (Geffen et al., 1976; Rice et al., 1994, 1997; Jaffe et al., 1998; Chen and Rice, 2001). Locally released DA in midbrain activates D2 DA autoreceptors that inhibit DA neuron firing via G-protein-coupled inwardly rectifying K^+ channels (GIRKs; Lacey et al., 1988; Beckstead et al., 2004, 2007; Courtney et al., 2012; Hikima et al., 2021). This process requires SNARE proteins, including SNAP-25 (Bergquist et al., 2002; Fortin et al., 2006; Hikima et al., 2021) and related RIM (Rab-interacting molecule) proteins (Robinson et al., 2019). Many other molecular aspects of somatodendritic release, however, are poorly understood.

Previous studies showed that somatodendritic DA release operates at submillimolar Ca^{2+} concentrations that do not support axonal DA release (Chen and Rice, 2001; Fortin et al., 2006;

Received Dec. 7, 2021; revised Feb. 18, 2022; accepted Mar. 18, 2022.

Author contributions: T.H., P.W., M.V.C., and M.E.R. designed research; T.H., P.W., and L.K. performed research; T.H., P.W., and L.K. analyzed data; T.H., P.W., and M.E.R. wrote the paper.

This work was supported by the Marlene and Paolo Fresco Institute for Parkinson's and Movement Disorders (to T.H. and M.E.R.), and National Institutes of Health Grants DA-050165 (to M.E.R.), MH-110136 (to M.V.C.), and NS-107616 (to M.V.C.). We thank Dr. Wade G. Regehr for donating Syt7 knock-out mice as founders for our colony.

The authors declare no competing financial interests.

Correspondence should be addressed to Margaret E. Rice at margaret.rice@nyu.edu.

https://doi.org/10.1523/JNEUROSCI.2416-21.2022

Chen et al., 2011; Mendez et al., 2011). In part, this involves contributions from intracellular Ca^{2+} stores (Patel et al., 2009; Hikima et al., 2021), but other factors may contribute, including a high-affinity Ca^{2+} sensor for exocytotic release. Intracellular Ca^{2+} sensing for transmitter release is achieved primarily by synaptotagmins (Syts), transmembrane proteins with two cytosolic Ca^{2+} binding (C2) domains (Südhof and Rizo, 1996). Messenger RNAs for Syt1, Syt4, Syt7, and Syt11 are found in SNc DA neurons (Glavan and Zivin, 2005; Mendez et al., 2011). Of these, Syt1 and Syt7 have Ca^{2+}-binding C2 domains, with Syt1 having low Ca^{2+} affinity and Syt7 having high Ca^{2+} affinity (Sugita et al., 2002; Pinheiro et al., 2016). Previous work has shown that Syt1 mediates fast, synchronous transmitter release (Geppert et al., 1994; Xu et al., 2007), including axonal DA release in dorsal striatum (Banerjee et al., 2020; Delignat-Lavaud et al., 2021). High-affinity Syt7 also contributes to asynchronous exocytotic release in neurons and secretory cells (Gustavsson et al., 2009; Jackman et al., 2016; Chen et al., 2017; Luo and Südhof, 2017). Previous evidence suggests that Syt7 is associated with the plasma membrane, in contrast to vesicle-associated Syt1 (Sugita et al., 2001), supporting differential roles for these Syts in Ca^{2+}-dependent exocytosis. Indeed, in endocrine cells that express both Syt1 and Syt7, the deletion of either Syt affects distinct components of exocytotic release (Schonn et al., 2008). Syt7 is a good candidate to mediate the high Ca^{2+} sensitivity of somatodendritic DA release, as supported by studies in cultured DA neurons (Fortin et al., 2006; Mendez et al., 2011).

We reported previously that D2 autoreceptor-dependent regulation of a given SNc DA neuron is governed primarily by DA released from that same cell (Hikima et al., 2021). This allows mechanistic studies of the release process through the application of antibodies or toxins via the pipette used to monitor DA-dependent D2 receptor-mediated inhibitory currents (D2ICs). Here, we report that in *ex vivo* midbrain slices, single-cell application of an antibody against Syt7 (Syt7 Ab) decreased the amplitude of D2ICs evoked in SNc DA neurons by brief pulse trains. Intracellular Syt7 Ab in wild-type (WT) SNc DA neurons also eliminated train-evoked DA release in submillimolar extracellular Ca^{2+} ($[Ca^{2+}]_o$), and attenuated D2IC amplitudes in $[Ca^{2+}]_o$ up to 2.4 mM $[Ca^{2+}]_o$. Loss of submillimolar Ca^{2+} sensitivity was also seen in Syt7 knock-out (KO) mice. Moreover, with changes in $[Ca^{2+}]_o$ in the millimolar range, Syt7 deletion had a greater effect on pulse-train (phasic) than on single-pulse (tonic) evoked DA release. Given that DA release persisted in millimolar $[Ca^{2+}]_o$ in Syt7 KOs, we tested a role for another Ca^{2+} sensor, Syt1. Although intracellular Syt1 Ab had no effect on train-evoked D2ICs in WT DA neurons, it caused a progressive decrease in D2IC amplitude in Syt7 KO cells. In addition, intracellular Syt1 Ab decreased single-pulse D2ICs in WT DA neurons. These data indicate that Syt1 influences tonic somatodendritic DA release, and provides functional substitution for normally dominant Syt7. Our findings establish that both Syt1 and Syt7 act as Ca^{2+} sensors for tonic and phasic aspects of somatodendritic DA release.

Materials and Methods

Animals. All animal procedures conform to guidelines of the Institutional Animal Care and Use Committee at the New York University Grossman School of Medicine. Both male and female mice were used at postnatal weeks 4–8; strains were C57BL/6J WT mice (stock no. 000664, The Jackson Laboratory) and Syt7 KO mice (Chakrabarti et al., 2003; Jackman et al., 2016; stock no. 004950, The Jackson Laboratory). All mice were group housed with controlled temperature and humidity, and maintained on a 12 h light/dark cycle (lights on at 6:30 A.M.) with food and water available *ad libitum* in an Association for Assessment and Accreditation of Laboratory Animal Care International-accredited facility. We did not observe any overt behavioral abnormalities in 4- to 8-week-old Syt7 KO mice. The initial report describing these mice indicated that they were born with the expected Mendelian ratio, with no gross abnormalities or obvious neurologic defects (Chakrabarti et al., 2003). On the other hand, subtle differences have been reported in slightly older Syt7 KO mice (age, 3–6 months), including bipolar-like behavioral fluctuations during the light/dark cycle (Shen et al., 2020).

Slice preparation. Mice were injected intraperitoneally with Euthasol (120 mg/kg pentobarbital), then perfused transcardially with ice-cold cutting solution containing the following (in mM): 200 sucrose; 2.5 KCl; 26 $NaHCO_3$; 1.25 NaH_2PO_4; 0.5 $CaCl_2$; 7 $MgSO_4$; 1 ascorbic acid; 3 sodium pyruvate; and 7 glucose. The solution was equilibrated with 95% O_2/5% CO_2 (Lee et al., 2013). Brains were removed and placed in ice-cold cutting solution for ~1 min. Horizontal midbrain slices (250 µm thick) were cut on a vibrating microtome (model VT1200S, Leica Microsystems), transferred to a holding chamber for 40 min at 35°C, and maintained for at least 30 min at room temperature in artificial CSF (aCSF) containing the following (in mM): 125 NaCl; 2.5 KCl; 25 $NaHCO_3$; 1.25 NaH_2PO_4; 2 $CaCl_2$; 1 $MgSO_4$; 1 sodium ascorbate; 3 sodium pyruvate; 25 glucose; and 0.4 myo-inositol (Lee et al., 2013). Experimental slices were transferred to the recording chamber and superfused at 1.2 mL/min with 32°C bicarbonate-buffered aCSF, containing the following (in mM): 124 NaCl; 3.7 KCl; 26 $NaHCO_3$; 2.4 $CaCl_2$; 1.3 $MgSO_4$; 1.3 KH_2PO_4, and 10 glucose, equilibrated with 95% O_2/5% CO_2. Experiments were conducted in 2.4 mM $[Ca^{2+}]_o$, except for those in which the Ca^{2+} dependence of somatodendritic DA release was assessed by changing $[Ca^{2+}]_o$ from 2.4 to 0.6, 1.2, or 3.6 mM, as the experiment dictated.

Electrophysiology. Evoked D2ICs were recorded in voltage-clamp mode using a Multiclamp 700B microelectrode amplifier with a Digidata 1550B converter and Clampex10.7 software (Molecular Devices). The medial terminal nucleus of the accessory optic tract was used as an anatomic landmark to identify the SNc in horizontal midbrain slices; SNc DA neurons were recognized by their large spindle-shaped cell bodies under infrared-differential interference contrast optics on a microscope (model BX50WI, Olympus America). The identity of DA neurons was then confirmed physiologically by their low spontaneous spike rate (1–5 Hz), action potential width of >1.2 ms, and the presence of an h-current (>200 pA) evoked in response to a membrane voltage step from −60 to −110 mV (Ford et al., 2006).

To record D2ICs, neurons were held at −60 mV; currents were filtered at 2 kHz and digitized at 10 kHz; and pipette resistance was 2.0–3.5 MΩ. The usual pipette solution contained the following (in mM): 115 K-methylsulfate; 20 NaCl; 1.5 $MgCl_2$; 5 HEPES; 10 EGTA; 3 Na_2-ATP; and 0.3 Na_3-GTP, at pH 7.3 with KOH, and 291–300 mOsm (Ford et al., 2010). For pharmacological isolation of D2ICs, picrotoxin (100 µM), CGP55845 (0.3 µM), 6,7-dinitroquinoxaline-2,3-dione DNQX; 10 µM) and D(−)-2-amino-phosphonopentanoic acid (D-AP5; 50 µM) were included in the recording aCSF (Beckstead et al., 2004; Hikima et al., 2021). Electrodes were prepared from glass capillaries (Sutter Instrument) with a horizontal micropipette puller (model P-97, Sutter Instrument). Series resistances were not compensated, and recordings were discarded if the series resistance exceeded 15 MΩ. A bipolar stimulating electrode (FHC) was placed on the slice surface, 50–100 µm lateral to a patched neuron. In most experiments, D2ICs were evoked by five-pulse trains at 40 Hz or single pulses applied at 4 min intervals. In some experiments, however, five-pulse trains and one-pulse stimulation were alternated at 2 min intervals in a given DA neuron to mimic phasic and tonic DA neuron activity. Voltage-clamp recording of quinpirole-induced currents was used to assess D2 receptor and GIRK channel function. Given that quinpirole can desensitize D2Rs (Robinson et al., 2017), we used an optimized quinpirole concentration (250 nM) and application time (15 s) to achieve a reproducible current that did not affect subsequent evoked D2ICs (Hikima et al., 2021).

For initial studies of the possible involvement of Syt7 in somatodendritic DA release, pulse train-evoked D2ICs were recorded with single-cell application of Syt7 Ab (5 or 10 µg/mL) or Syt1 Ab (10 µg/mL) via

Table 1. Immunohistochemical reagents

Antibody	Animal	Source	Catalog #	Dilution
Syt7	Rabbit	Synaptic Systems	105173	1:1000
Syt1	Guinea pig	Synaptic Systems	105015	1:1000
TH	Sheep	Abcam	ab113	1:1000
Syt7 blocking peptide		Synaptic Systems	105-71P	1:1000
Syt1 blocking peptide		Synaptic Systems	105-01P	1:1000
Cy3 anti-rabbit	Donkey	The Jackson Laboratory	711–165-152	1:200
Cy3 anti-guinea pig	Donkey	The Jackson Laboratory	706–005-148	1:200
Cy5 anti-sheep	Donkey	The Jackson Laboratory	713–175-147	1:200

the recording pipette. After patching a given cell, the Ab infiltrated the cell by diffusion. The Syt 7Ab used (Synaptic Systems; Table 1) was raised against amino acid residues 46–133 of the Syt7 intracellular region. Specificity of Syt7 was supported by the absence of immunostaining after preadsorption with its blocking peptide (BP; Synaptic Systems; Fig. 1*A*) and confirmed by the absence of staining in brain sections from Syt7 KO mice (Fig. 1*B*), or in Western blots of tissue from Syt7 KOs (Fig. 1*C*), as seen in previous studies (Jackman et al., 2016; Chen et al., 2017). Initial D2ICs were recorded within 5 min of patching and monitored until a stable maximal effect was seen (final D2IC; 32–36 min). Control measurements with Syt7 Ab plus its blocking peptide or a nonspecific Ig (IgG) were time-matched to the duration required for Syt7 Ab alone. To examine a role for Syt1, we used both a Syt1 Ab (Synaptic Systems; Table 1) that was raised against amino acid residues 405–421 of the Syt1 intracellular region and its blocking peptide. Stock Syt7 Ab and Syt1 Ab solutions were diluted in the pipette solution. In some experiments, Neurobiotin 488 (0.01%; catalog #SP-1125–2, Vector Laboratories) was included with Syt7 Ab or Syt1 Ab to mark recorded neurons.

Immunohistochemistry. Mice were administered Euthasol intraperitoneally, then perfused transcardially with PBS followed by freshly prepared 4% paraformaldehyde (PFA) in 0.1 M PBS, pH 7.2. Brains were removed, postfixed in PFA overnight at 4°C, and cryoprotected in 20% and then 30% sucrose. Frozen coronal sections (50 µm thick) were cut through SNc using a Cryocut 1800 cryostat (Belair Instrument) and processed for immunohistochemistry. Brain sections were washed 3-× 15 min in PBS + 0.1% Triton X-100, then 1 h in 5% donkey serum in PBS + 0.3% Triton X-100. Thereafter, sections were incubated in primary antibodies for 18–24 h at room temperature on a shaking platform. Primary antibodies for Syt7, Syt1, and tyrosine hydroxylase (TH) and the secondary antibodies used are listed in Table 1 with their catalog numbers and working dilutions. Following 3× 15 min washes in PBS, sections were incubated in fluorescent secondary antibodies diluted 1:200 for 2 h. After 3× 15 min final washes in PBS alone, sections were mounted on slides, air dried, dehydrated in graded alcohols, treated with CitriSolv, and coverslipped with Krystalon (Millipore Sigma). Experimental midbrain slices in which Neurobiotin was used to identify neurons recorded with Syt7 Ab in the pipette were fixed overnight in PFA, then the whole slice was processed as described above, except that the dehydration and CitriSolv steps were omitted and the slice was mounted in VectaShield (Vector Laboratories).

Images of immunostained tissue were obtained with a confocal microscope (model Eclipse C1, Nikon) and processed with Photoshop (Adobe Systems). Any changes in brightness and/or contrast were made on the entire image. Control experiments included incubation for 2–12 h at 1:1 with the blocking peptide, resulting in the loss of specific immunostaining [Fig. 1*A* (see also Fig. 7*A*)]. Comparisons of immunostained control and preabsorbed tissue were made on adjacent sections from the same brain, using identical confocal photomultiplier settings. Each primary antibody and blocking peptide was tested on at least four mice.

Western blotting. To obtain tissue samples for immunoblotting, mice were administered Euthasol intraperitoneally and decapitated, and the brains were removed into ice-cold PBS. Individual regions were dissected and frozen immediately on dry ice. Samples were maintained at −80°C until processed. The methods used for immunoblotting were similar to those used previously (Sathler et al., 2021). Tissue samples were homogenized in radioimmunoprecipitation buffer (50 mM Tris-HCl, pH 7.4, 150 mM NaCl, 1% Nonidet P40, 0.5% deoxycholate, 0.1% SDS, and 10 mM EGTA) with phosphatase and protease inhibitors (Roche). Equal amounts of protein (20 µg) were loaded on 10% SDS-PAGE gels and transferred to nitrocellulose membranes, which were blotted with Syt7 (1:2000) or Syt1 Ab (1:2000), and β-actin (1:5000; catalog #3700S, Cell Signaling Technology). Secondary antibodies were used at 1:5000 dilution: goat anti-rabbit-HRP (catalog #G21234, Thermo Fisher Scientific), goat anti-mouse-HRP (catalog #31439, Thermo Fisher Scientific), and donkey anti-guinea pig-HRP (catalog #706036148, Jackson ImmunoResearch).

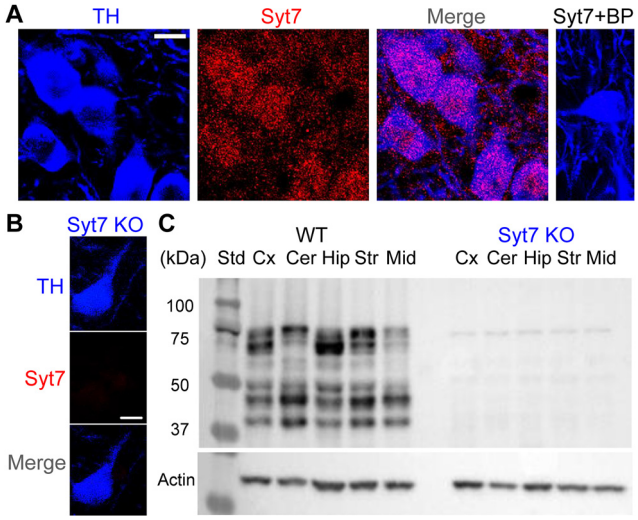

Figure 1. Syt7 immunoreactivity in SNc DA neurons and efficacy of Syt7 KO. ***A***, Representative images showing immunostaining for Syt7 (red) and TH (blue) in the SNc of a coronal midbrain section in WT mice. Preadsorption of Syt7 with its BP resulted in loss of Syt7 immunostaining (Syt7+BP). Scale bar, 10 µm. ***B***, Representative images showing immunostaining for Syt7 and TH in the SNc of a coronal midbrain section in Syt7 KO mice. Scale bar, 10 µm. ***C***, Immunoblot of brain region extracts from WT or homozygous Syt7 KO mice probed with an affinity-purified antibody against the Syt7 confirms specificity of the Syt7 Ab and the efficacy of the KO. Cx, Cortex; Cer, cerebellum; Hip, hippocampus; Str, striatum; Mid, midbrain; Std, protein molecular mass standard.

Chemicals. EGTA, BAPTA, and picrotoxin were purchased from Millipore Sigma; D-AP5, DNQX, CGP55845, sulpiride, and quinpirole were from Tocris Bioscience. Other salts, including $CaCl_2$, were from Millipore Sigma.

Analysis and statistics. Electrophysiological data were obtained and quantified using pClamp10 (Molecular Devices), then analyzed and graphed with Clampfit (Molecular Devices) and GraphPad Prism (GraphPad Software). These data are reported as the mean ± SEM (*n*, number of cells). Kinetic parameters for D2IC were determined from an average of at least three measurements per cell. The time to peak was measured from the end of the last stimulation pulse to the peak of the evoked D2IC. Half-width was a measure of D2IC duration, calculated as the difference between the time points at 50% of peak D2IC amplitude on the rising and falling phases. Decay time was estimated from an exponential function used to fit the falling phase of D2ICs. To determine the Ca^{2+} cooperativity (Hill coefficient) and Ca^{2+} sensitivity (EC_{50}) for each condition, normalized D2IC amplitude data in each $[Ca^{2+}]_o$ was analyzed using the Hill equation (Schneggenburger and Neher, 2000). Differences for within-group comparisons were assessed by paired two-tailed *t* tests. Differences among three experimental groups were determined by two-way ANOVA and Holm–Sidak multiple-comparisons tests. For all data, statistical significance was considered to be $p < 0.05$.

Results

Identification of Syt7 in SNc DA neurons

Previous work documented the expression of Syt7 mRNA in rat DA neurons and Syt7 protein in cultured mouse DA cells (Glavan and Zivin, 2005; Mendez et al., 2011). Here we identified

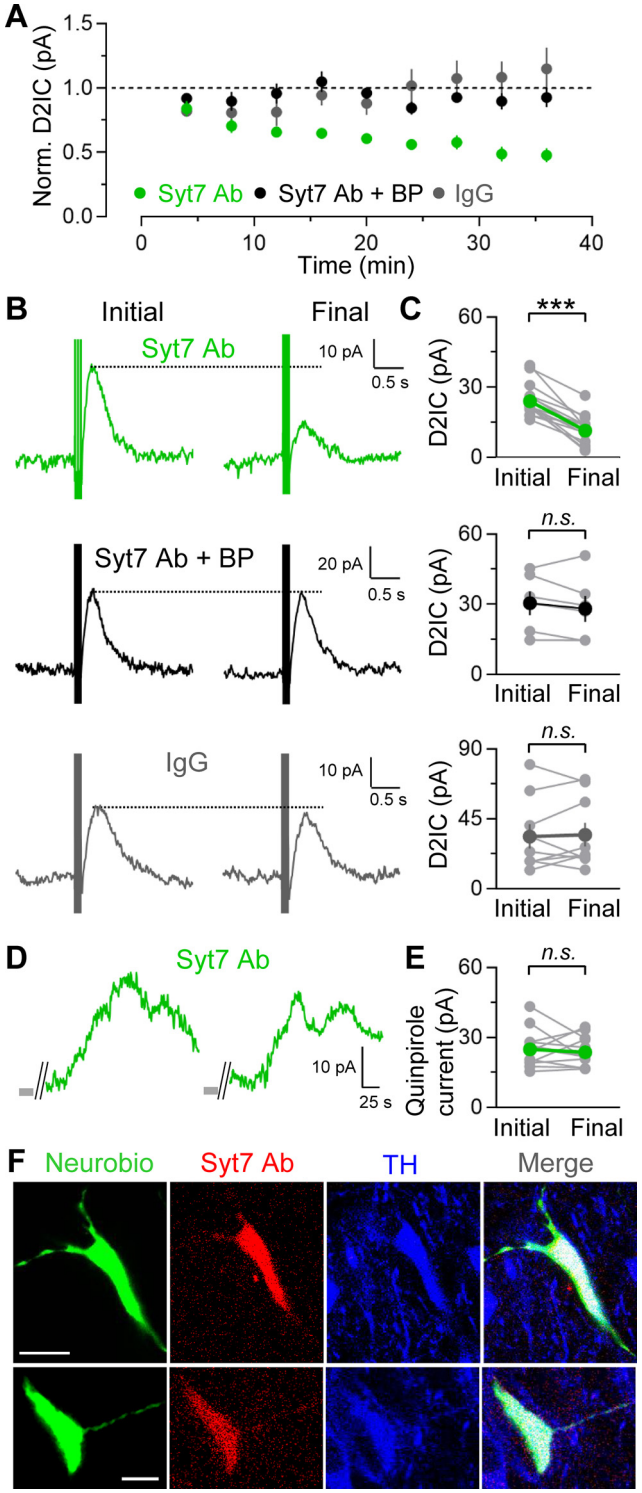

Figure 2. Intracellular application of Syt7 Ab decreases D2IC amplitude. ***A***, Average time course of changes in the amplitude of phasic D2ICs (five pulses, 40 Hz) with Syt7 Ab, Syt7 Ab+BP, or IgG in the recording pipette. Intracellular application of Syt7 Ab alone decreased amplitude; coinfusion of the BP for Syt7 Ab nullified this effect. ***B***, Representative D2ICs after establishing whole-cell recording (initial) and at the end of the recording period (final). ***C***, Quantification of D2IC amplitude when recorded with Syt7, Syt7 Ab+BP, or IgG (Syt7 Ab: final, 48 ± 5% of initial, $n = 15$; Syt7 Ab+BP: final, 91 ± 6% of initial, $n = 6$; $p = 0.26$; IgG: final, 111 ± 14% of initial, $n = 9$; $p = 0.74$, paired t test). ***D***, Representative D_2-dependent currents evoked by brief superfusion of quinpirole (250 nM, 15 s). Quinpirole was applied immediately after establishing whole-cell recording (initial) and at the end of the recording period (final) with Syt7 Ab in the pipette. ***E***, Quantification of quinpirole-evoked D2 currents in the presence of Syt7 (Syt7 Ab: final, 99 ± 8% of initial, $n = 12$; $p = 0.66$, paired t test). ***F***, Representative immunostaining of Syt7 Ab and TH in the SNc in two horizontal slices after whole-cell recording. Neurobiotin 488 was used to identify patch-clamped cells and was introduced together with Syt7 Ab via the recording pipette ($n = 6$ slices). Scale bars, 10 µm. n.s., Not significant. ***$p < 0.0001$.

Syt7 in SNc DA neurons in mouse brain sections using immunohistochemistry; Syt7 immunoreactivity was readily detected in DA cell bodies and dendrites identified by TH immunoreactivity (sections from four mice) and was absent either when the Syt7 Ab was preincubated with its blocking peptide (Fig. 1*A*) or in Syt7 KO mice (Fig. 1*B*). Additionally, the specificity of the Syt7 Ab used was confirmed in immunoblotting experiments against proteins from diverse brain regions in both WT and Syt7 KO mice (Fig. 1*C*). Consistent with earlier studies (Sugita et al., 2001; Chakrabarti et al., 2003; Schonn et al., 2008), Syt7 Ab immunostained multiple bands ranging from 45 to 90 kDa in cortex, cerebellum, hippocampus, striatum, and midbrain. In contrast, immunoblots of the same brain regions from Syt7 KOs were devoid of immunostaining, confirming both the absence of Syt7 in KO mice and the specificity of the Syt7 Ab (Fig. 1*C*).

Single-cell application of Syt7 Ab attenuates somatodendritic DA release

Somatodendritic DA release can be studied by monitoring the D2ICs resulting from D2 autoreceptor activation by DA released from the recorded cell during local stimulation (Beckstead et al., 2004, 2007; Ford et al., 2010; Courtney et al., 2012; Gantz et al., 2013; Hikima et al., 2021). Here we tested a possible functional role for Syt7 in somatodendritic DA release by examining the effect of intracellular application of our validated Syt7 Ab on the amplitude of evoked D2ICs. In initial experiments, D2ICs were evoked by brief, phasic stimulation (40 Hz, five pulses; Beckstead et al., 2004; Hikima et al., 2021). Both male and female WT and Syt7 KO mice were studied. We found no sex differences in the physiological properties used to identify SNc DA neurons (WT: spontaneous spike rate: males, 2.8 ± 0.2 Hz, $n = 25$; females, 3.2 ± 0.4 Hz, $n = 11$; $p = 0.49$; h-current: males, 833 ± 56 pA, $n = 25$; females, 1041 ± 115 pA, $n = 11$; $p = 0.08$; D2IC amplitude: males, 39.8 ± 4.4 pA, $n = 17$; females, 38.0 ± 4.0 pA, $n = 8$; $p = 0.80$, unpaired t test; Syt7 KO: spontaneous spike rate: males, 2.8 ± 0.2 Hz, $n = 26$; females, 3.3 ± 0.4 Hz, $n = 9$; $p = 0.30$; h-current: males, 832 ± 64 pA, $n = 27$; females, 954 ± 89 pA, $n = 9$; $p = 0.34$; D2IC amplitude: males, 33.6 ± 2.2 pA, $n = 27$; females, 26.3 ± 1.9 pA, $n = 8$; $p = 0.07$, unpaired t test). Subsequently, data from both sexes were pooled. Single-cell application of Syt7 Ab (10 µg/mL) caused a decrease in D2IC amplitude that reached a stable minimum after ~30 min (Fig. 2*A–C*; D2IC amplitude with Syt7Ab: 48 ± 5% of initial, $n = 15$; $p < 0.0001$, paired t test). In contrast, the final amplitude of evoked D2ICs following coapplication of Syt7 Ab with its blocking peptide (20 µg/mL) or, alternatively, with a nonspecific IgG, did not differ from initial amplitude over the same recording period (Syt7 Ab + BP: final, 91 ± 6% of initial, $n = 6$; $p = 0.26$; IgG: final, 111 ± 14% of initial, $n = 9$; $p = 0.74$, paired t tests; Fig. 2*A–C*).

To assess the possible influence of Syt7 Ab on D2 receptor or GIRK channel function, we evaluated the effect of each experimental condition on D2 receptor currents elicited by external application of quinpirole, a D2 receptor agonist (Hikima et al., 2021). Given that D2 receptors can desensitize with agonist application in a Ca^{2+}-dependent manner (Robinson et al., 2017), we compared the stability of quinpirole-activated currents with

EGTA- or BAPTA-based internal solutions. Superfusion of quinpirole (250 nM) at the beginning of recording for 15 s produced D2 currents in the same amplitude range as evoked D2ICs with either internal solution (Fig. 2*D*,*E*). A second application at the end of the experiment revealed that quinpirole-induced currents were stable over the recording period with Syt7 Ab in either internal solution (EGTA: second application, 107 ± 12% of initial, $n = 5$; BAPTA: second application, 94 ± 9% of initial, $n = 7$; $p = 0.41$, unpaired t tests; Fig. 2*D*,*E*). These data were therefore pooled. The similarity of initial and final quinpirole current amplitudes indicates that the decrease in evoked D2IC amplitude with intracellular Syt7 Ab reflects a decrease in DA release, and does not occur because of altered D2 receptor sensitivity or impaired GIRK channel function.

To confirm the single-cell specificity of pipette application, we used immunohistochemical staining with a secondary antibody to localize Syt7 Ab in a subpopulation of recorded neurons ($n = 5$). The tested cells were filled with Neurobiotin 488 and were subsequently identified as DA neurons by immunoreactivity for TH. In these experiments, five of five recorded cells showed immunostaining for both Syt7 Ab (secondary Ab only) and TH. The pattern of staining confirmed that Syt7 Ab infiltrated the soma and proximal dendrites of DA neurons during the time of recording and that the Syt7 Ab was confined to the recorded cell (Fig. 2*F*). For our previous study using single-cell Ab or toxin application, we conducted a series of control experiments to confirm that the effects seen were from intracellular application and not extracellular leakage (Hikima et al., 2021). In one of these experiments, we used positive pressure to eject an Ab (against SNAP-25) near a DA neuron, then recorded from that cell with a pipette lacking that Ab. We found no change in evoked D2IC amplitude following extracellular Ab application, whereas intracellular application caused a consistent, significant decrease (Hikima et al., 2021, their Fig. S5), demonstrating the selectivity and efficacy of our single-cell application method.

We further examined the influence of Syt7 Ab on D2IC kinetics, including time to peak, half-width, and decay time. The time to peak D2IC amplitude was increased with intracellular application of Syt7 Ab (Fig. 3*A*–*C*; Syt7 Ab: initial, 204 ± 10 ms; final, 265 ± 13 ms, n = 7; $p = 0.004$, paired t test), without a change in half-width or decay time (half-width: initial, 359 ± 9 ms; final, 369 ± 15 ms; $p = 0.57$; decay time constant: initial, 396 ± 25 ms; final, 412 ± 37 ms, n = 7; $p = 0.73$, paired t test). Given the lack of change in the overall D2IC time course, which is governed primarily by D2–GIRK kinetics (Beckstead et al., 2007), the increased time to reach peak amplitude presumably reflects the decreased influence of Syt7 on the release process. Increased time to peak is unlikely to result from reduced DA release, as we previously found no correlation between peak amplitude and time to peak in D2ICs recorded under control conditions (Hikima et al., 2021). None of these D2IC kinetic properties was altered by intracellular coapplication of the blocking peptide with Syt7 Ab or by IgG alone (Fig. 3*A*–*C*).

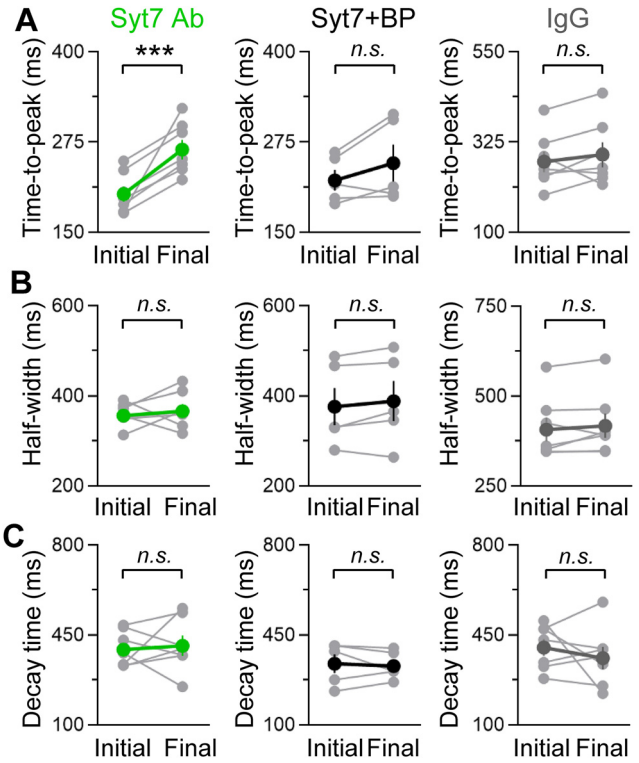

Figure 3. Intracellular application of Syt7 Ab in SNc DA neurons delayed the time to peak of evoked D2ICs compared with controls, but did not alter other D2IC parameters. ***A***, Time to peak (Syt7 Ab: initial, 204 ± 10 ms; final, 265 ± 13 ms, $n = 7$; $p = 0.004$; Syt7 Ab+BP: initial, 196 ± 7 ms; final, 208 ± 2 ms, $n = 5$; $p = 0.15$; IgG: initial, 278 ± 24 ms; final, 296 ± 29 ms, $n = 7$; $p = 0.35$). ***B***, Half-width (duration at 50% peak amplitude): Syt7 Ab: initial, 359 ± 9 ms; final, 369 ± 15 ms; $p = 0.56$; Syt7 Ab+BP: initial, 310 ± 20 ms; final, 318 ± 20 ms; $p = 0.22$; IgG: initial, 410 ± 30 ms; final, 421 ± 31 ms; $p = 0.32$). ***C***, Decay time constant (Syt7 Ab: initial, 396 ± 25 ms; final, 412 ± 37 ms; $p = 0.73$; Syt7 Ab+BP: initial, 304 ± 24 ms; final, 268 ± 20 ms; $p = 0.69$; IgG: initial, 405 ± 31 ms; final, 364 ± 41 ms; $p = 0.44$, paired t test). n.s., Not significant. ***$p < 0.001$.

Calcium dependence of somatodendritic DA release

We assessed the influence of Syt7 on the Ca^{2+} dependence of somatodendritic DA release, as indexed by relative changes in D2IC amplitude in varying $[Ca^{2+}]_o$ (Fig. 4). In SNc DA neurons from WT mice, evoked D2ICs were readily detected in submillimolar $[Ca^{2+}]_o$ (Fig. 4*A*). Peak D2IC amplitude relative to that in 2.4 mM $[Ca^{2+}]_o$ was 72 ± 6% in 1.2 mM $[Ca^{2+}]_o$ ($n = 6$) and 48 ± 12% in 0.6 mM ($n = 6$; Fig. 4*B*,*C*). These results are consistent with prior observations using fast-scan cyclic voltammetry (FSCV; Chen and Rice, 2001; Chen et al., 2011). We next examined the effect of intracellular Syt7 Ab (5 μg/mL) on the Ca^{2+} dependence of evoked D2ICs. In 3.6 mM $[Ca^{2+}]_o$, the amplitude of D2ICs recorded with intracellular Syt7 Ab did not differ from that in WT mice under control conditions (Fig. 4*A*–*C*). However, D2ICs in 0.6 and 1.2 mM $[Ca^{2+}]_o$ were significantly lower with Syt7 Ab in the pipette than in WT controls (1.2 mM $[Ca^{2+}]_o$, $p = 0.042$, WT vs WT+Syt7 Ab; 0.6 mM $[Ca^{2+}]_o$, $p = 0.011$, WT vs WT+Syt7 Ab; two-way ANOVA with Holm–Sidak multiple-comparisons tests; Fig. 4*B*,*C*). Indeed, D2ICs evoked with Syt7 Ab were nearly abolished in 0.6 mM $[Ca^{2+}]_o$ (1.2 mM $[Ca^{2+}]_o$, 48 ± 12% of 2.4 mM $[Ca^{2+}]_o$, $n = 6$; D2IC amplitude in 0.6 mM $[Ca^{2+}]_o$, 8 ± 6% of 2.4 mM $[Ca^{2+}]_o$, $n = 6$; Fig. 4*A*–*C*). A similar pattern was seen for the Ca^{2+} dependence of DA release in SNc DA neurons from Syt7 KO mice, as follows: D2IC amplitude between KO and WT mice was similar at 3.6 mM $[Ca^{2+}]_o$, but the amplitude for Syt7 KOs was significantly smaller than in WT mice at 1.2 mM $[Ca^{2+}]_o$ and was, again, nearly absent at 0.6 mM $[Ca^{2+}]_o$ (Syt7 KO: D2IC amplitude in 3.6 mM $[Ca^{2+}]_o$, 117 ± 3% of 2.4 mM $[Ca^{2+}]_o$, $n = 4$; D2IC amplitude in 1.2 mM $[Ca^{2+}]_o$, 39 ± 13% of 2.4 mM $[Ca^{2+}]_o$, $n = 6$; D2IC amplitude in 0.6 mM $[Ca^{2+}]_o$, 13 ± 6% of 2.4 mM $[Ca^{2+}]_o$, $n = 6$; Fig. 4*A*–*C*).

Estimation of Ca^{2+} sensitivity and cooperativity for somatodendritic DA release

The Ca^{2+} dependence of D2ICs recorded in SNc DA neurons from WT mice, from WT mice with Syt7 Ab, or from Syt7 KOs

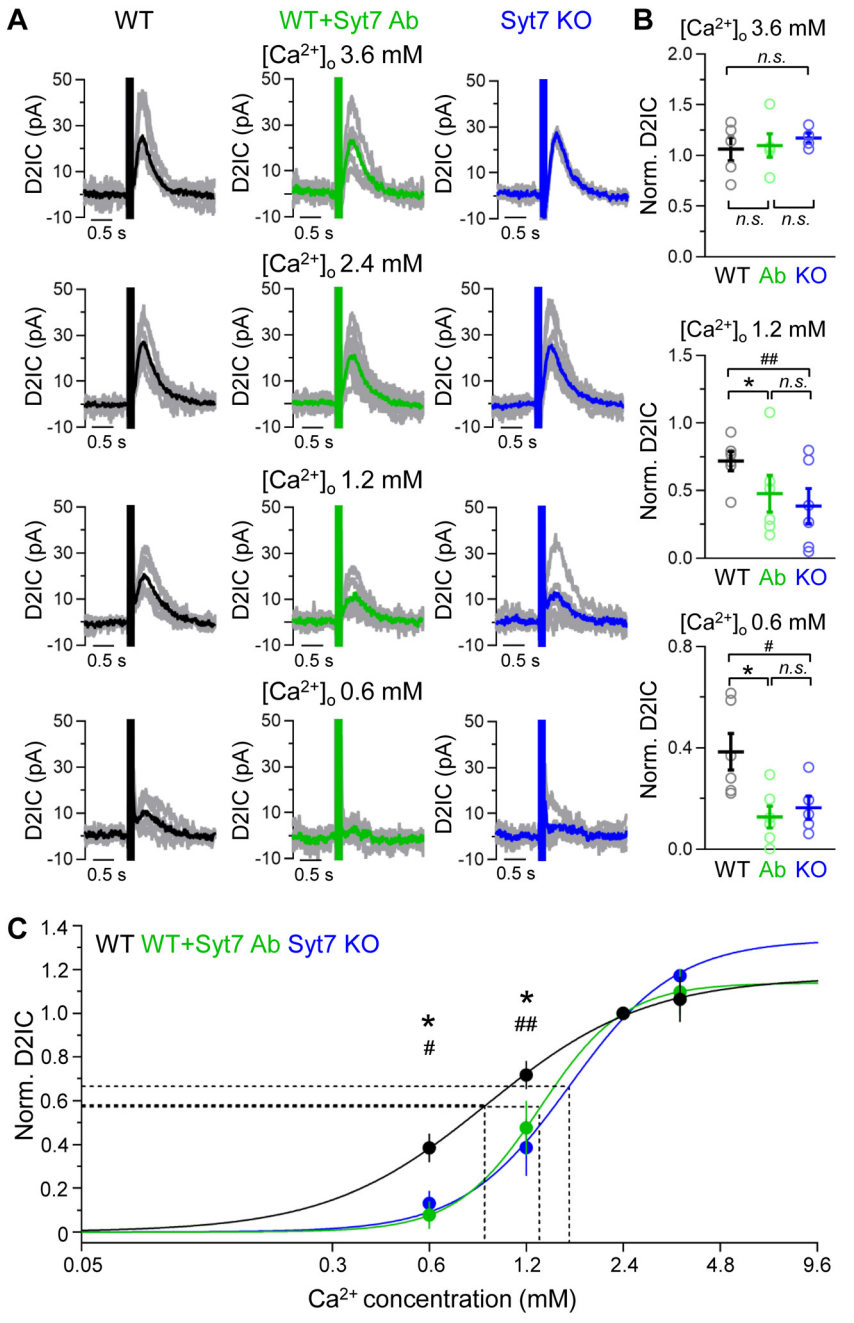

Figure 4. Influence of Syt7 on the Ca^{2+} dependence of somatodendritic DA release. ***A***, Evoked D2ICs in the SNc in varying $[Ca^{2+}]_o$. Averaged records are shown in color, and single D2IC traces are shown in gray. In control WT SNc DA neurons, robust D2ICs were seen in 1.2 and 0.6 mM $[Ca^{2+}]_o$. However, D2ICs were minimal in low $[Ca^{2+}]_o$ when recorded with intracellular Syt7 Ab or in SNc DA neurons from Syt7 KO mice. ***B***, D2IC amplitudes from WT, WT+Syt7 Ab, and Syt7 KO SNc DA neurons normalized to D2IC amplitude in 2.4 mM $[Ca^{2+}]_o$ for each cell (3.6 mM: WT vs Ab, $p = 0.79$; WT vs KO, $p = 0.75$; Ab vs KO, $p = 0.79$; 1.2 mM: WT vs Ab, $p = 0.042$; WT vs KO, $p = 0.0054$; Ab vs KO, $p = 0.38$; 0.6 mM: WT vs Ab, $p = 0.011$; WT vs KO, $p = 0.042$; Ab vs KO, $p = 0.62$; $n = 4$–6/condition, two-way ANOVA with Holm–Sidak multiple-comparisons test). ***C***, Ca^{2+} dependence of somatodendritic DA release in SNc, normalized to peak amplitude in 2.4 mM $[Ca^{2+}]_o$ for each condition. Solid lines show the Hill fit for WT (black), Syt7 Ab in WT (green), and Syt7 KO (blue). The calculated Hill coefficients were 1.8 for WT, 3.3 for WT+Syt7 Ab, and 2.6 for Syt7 KO. The *x*-axis for each Hill plot was extended to 9.6 mM $[Ca^{2+}]_o$ to permit extrapolation of the Ca^{2+} dependence to an approximate maximal level for each region. These plots were also used to calculate the $[Ca^{2+}]_o$ at which DA release is half-maximal (EC_{50}), indicated by dashed lines: WT EC_{50} was 0.9 mM $[Ca^{2+}]_o$; WT+Syt7 Ab was 1.3 mM $[Ca^{2+}]_o$; and Syt7 KO was 1.6 mM $[Ca^{2+}]_o$ ($n = 4$–6 for each data point, two-way ANOVA with Holm–Sidak multiple-comparisons test). n.s., Nonsignificant. *$p < 0.05$, WT vs Syt7 Ab; #$p < 0.05$, WT vs Syt7 KO; ##$p < 0.01$, for WT vs Syt7 KO.

was evaluated by best-fit Hill plots (Fig. 4*C*). The $[Ca^{2+}]_o$ at which evoked D2IC amplitude was half-maximal (i.e., EC_{50}) for WT mice was 0.9 mM $[Ca^{2+}]_o$, but this increased to 1.3 mM with intracellular Syt7 Ab and to 1.6 mM in Syt7 KO mice. The calculated slope of the function (Hill coefficient) was used to estimate Ca^{2+} cooperativity. The estimated Hill coefficient for the WT data was 1.8, which is consistent with previous reports using FSCV to monitor DA release in the SNc (Chen et al., 2011). In contrast, the Hill plot of the Ca^{2+} dependence of DA release after intracellular Syt7 Ab application or in Syt7 KO mice yielded coefficients of 3.3 and 2.6, respectively. These data show that Syt7 modulates the Ca^{2+} dependence of somatodendritic DA release.

Greater influence of Syt7 on phasic than tonic somatodendritic DA release

In vivo, SNc DA neurons exhibit the following two distinct firing patterns: burst firing (phasic) and steady pacemaker activity (tonic; Grace and Bunney, 1984). Accordingly, we compared the role of Syt7 in the Ca^{2+} dependence of somatodendritic DA release evoked with a phasic pulse train (five pulses, 40 Hz) alternated, at 2 min intervals, with single-pulse stimulation in the same cell (Fig. 5*A*). In 2.4 mM $[Ca^{2+}]_o$, the amplitude of phasic D2ICs did not differ between WT and Syt7 KO mice (2.4 mM $[Ca^{2+}]_o$: WT, 36.9 ± 4.9 pA, $n = 9$; Syt7 KO, 32.0 ± 3.2 pA, $n = 8$; $p = 0.47$, unpaired *t* test) and neither did that of single-pulse evoked D2ICs (2.4 mM $[Ca^{2+}]_o$: WT: 11.4 ± 1.0 pA, $n = 9$; Syt7 KO: 13.0 ± 1.4 pA, $n = 8$; $p = 0.27$, unpaired *t* test). However, when $[Ca^{2+}]_o$ was decreased to 1.2 mM, a marked effect of Syt7 deletion was seen for phasic D2ICs, with significantly lower D2IC amplitude in DA cells from Syt7 KO versus WT mice (1.2 mM $[Ca^{2+}]_o$: WT: 27.9 ± 3.2 pA, $n = 9$; Syt7 KO: 14.6 ± 2.1 pA, $n = 8$; $p = 0.014$, unpaired *t* test). In contrast, there was no difference in D2IC amplitude between genotypes when evoked with single-pulse stimulation (1.2 mM $[Ca^{2+}]_o$: WT: 6.9 ± 0.7 pA, $n = 9$; Syt7 KO: 7.7 ± 0.7 pA, $n = 8$; $p = 0.49$, unpaired *t* test). The influence of Syt7 on the Ca^{2+} dependence of phasic DA release is seen in the ratio of D2IC amplitudes in 1.2 mM versus 2.4 mM $[Ca^{2+}]_o$ (Fig. 5*B*). Decreasing $[Ca^{2+}]_o$ had a significantly greater effect in Syt7 KO versus WT mice with five-pulse stimulation, whereas no genotypic difference was seen for one-pulse evoked D2ICs (Fig. 5*B*). These data suggest that the influence of Syt7 is greater on phasic than on tonic DA release. To examine this possibility directly, we compared the ratio of phasic-to-tonic D2IC

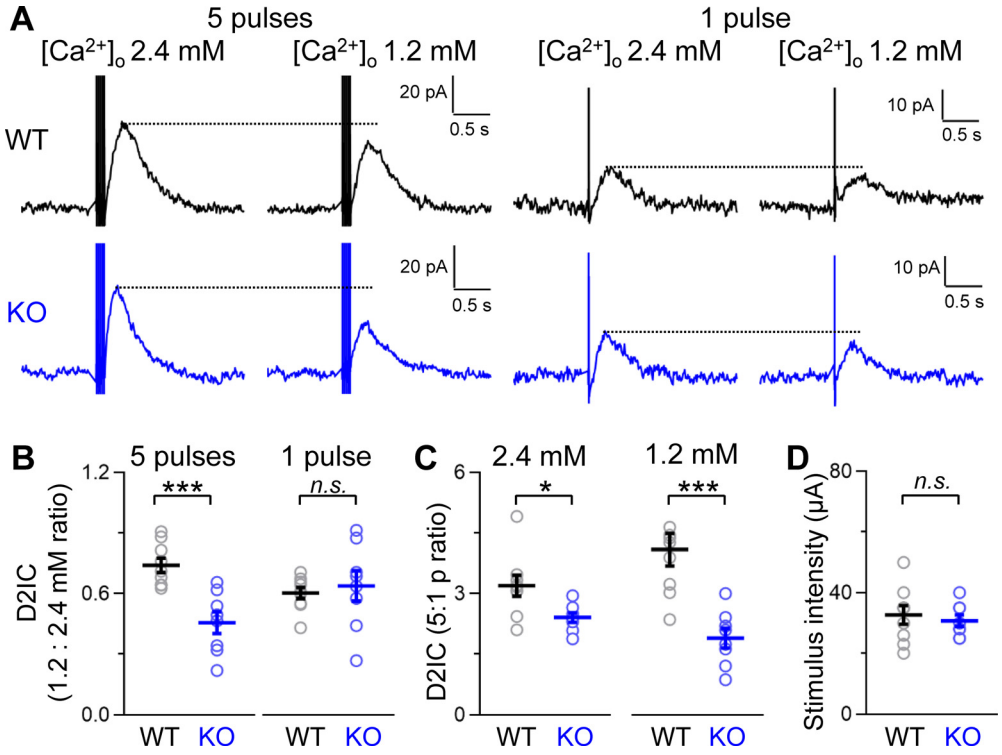

Figure 5. The influence of Syt7 on phasic versus tonic somatodendritic DA release. ***A***, Representative D2ICs elicited by one-pulse (tonic) or five-pulse (phasic) stimulation at 40 Hz in 2.4 or 1.2 mM $[Ca^{2+}]_o$ in SNc DA neurons from WT and Syt7 KO mice. ***B***, Ratio of D2IC amplitude in 1.2 mM $[Ca^{2+}]_o$ to 2.4 mM $[Ca^{2+}]_o$ as an index of the Ca^{2+} dependence in WT and Syt7 KO mice. The effect of decreasing Ca^{2+} on five-pulse evoked D2ICs was significantly greater in Syt7 KO mice versus WT, whereas no genotypic difference was seen with one-pulse evoked D2ICs (phasic D2ICs: WT, 1.2 mM 0.76 ± 0.03 of 2.4 mM, $n = 9$; Syt7 KO, 1.2 mM 0.46 ± 0.05 of 2.4 mM, $n = 8$; $p = 0.0004$; tonic D2ICs: WT, 1.2 mM 0.60 ± 0.03 of 2.4 mM, $n = 9$; Syt7 KO: 1.2 mM 0.64 ± 0.07 of 2.4 mM, $n = 8$; $p = 0.65$, unpaired *t* test). ***C***, Ratio of five-pulse to one-pulse (5:1 p ratio) evoked D2IC amplitude in a given SNc DA neuron shows that Syt7 amplifies the contrast between phasic and tonic somatodendritic DA release (2.4 mM: WT, 3.2 ± 0.2, $n = 9$; Syt7 KO, 2.5 ± 0.2, $n = 8$; $p = 0.018$; 1.2 mM: WT, 4.1 ± 0.4, $n = 9$; Syt7 KO, 1.9 ± 0.2, $n = 8$; $p = 0.0004$, unpaired *t* test). ***D***, Stimulation intensities used to evoked D2ICs did not differ between WT and Syt7 KO SNc DA neurons (WT: 33.0 ± 0.3 μA, $n = 9$; Syt7 KO: 31.0 ± 0.2 μA, $n = 8$; $p = 0.61$, unpaired *t* test). n.s., Not significant. $^*p < 0.05$, $^{***}p < 0.001$.

amplitude (5:1 pulse ratio) for each genotype and $[Ca^{2+}]_o$ (Fig. 5*C*). We found a significant decrease in the 5:1 pulse ratio in Syt7 KO versus WT mice in both 2.4 and 1.2 mM $[Ca^{2+}]_o$ (Fig. 5*C*). Stimulus intensity used in these measurements did not differ between recordings in Syt7 KO and WT mice (Fig. 5*D*), thus ruling out a potential variable. These data demonstrate a key role for Syt7 in amplifying the contrast between phasic and tonic somatodendritic DA release in physiologically relevant $[Ca^{2+}]_o$.

Functional replacement of Syt1 for somatodendritic DA release in Syt7 KO mice and influence of Syt1 on tonic DA release

Given the efficacy of Syt7 Ab in suppressing somatodendritic DA release in WT DA neurons in 2.4 mM $[Ca^{2+}]_o$ (Fig. 2*A–C*), the similarity of D2IC amplitudes evoked by phasic stimulation of SNc DA neurons from Syt7 KO and WT mice was surprising (Fig. 4*A*). We investigated possible explanations for this apparent anomaly, first by testing the stability of D2ICs in Syt7 KO mice. We observed that D2ICs evoked by phasic stimulation in neurons from Syt7 KO mice were stable over the standard recording period (final: 93 ± 14% of initial, $n = 4$; $p = 0.95$, paired *t* test; Fig. 6*A–C*). We also found no differences in the kinetics of D2ICs recorded in SNc DA neurons from Syt7 KO versus WT mice (Fig. 6*D–F*). Quinpirole-induced currents in KO mice also did not differ from those in WT (Fig. 6*G*; WT: 43.7 ± 5.3 pA, $n = 9$; KO: 41.6 ± 5.2 pA, $n = 10$; $p = 0.79$, unpaired *t* test), indicating unaltered D2 sensitivity or GIRK coupling after Syt7 deletion. Last, we found no differences in the basic physiological characteristics of SNc DA neurons from Syt7 KO versus WT mice (Fig. 6*H–L*).

The persistence of pulse train-evoked D2ICs after Syt7 deletion with sufficiently high $[Ca^{2+}]_o$ implies that DA release in Syt7 KOs requires an additional Ca^{2+} sensor. Previously reported evidence for Syt1 in SNc DA neurons (Glavan and Zivin, 2005), and the dependence of axonal DA release on Syt1 in the striatum (Banerjee et al., 2020; Delignat-Lavaud et al., 2021), led us to focus on a possible role for this Syt isoform. Immunostaining identified Syt1 protein in the somata and dendrites of SNc DA neurons (sections from five mice), which was absent when the Syt1 Ab was preincubated with its blocking peptide (Fig. 7*A*). We and others have reported the apparent absence of detectable Syt1 immunoreactivity in midbrain DA neurons (Witkovsky et al., 2009; Delignat-Lavaud et al., 2022). Our earlier study (Witkovsky et al., 2009) used an Ab against Syt1,2 that did not stain guinea pig midbrain DA neurons. In contrast, the specific anti-Syt1 Ab used in the present study also immunostained guinea pig SNc DA neurons, with the absence of staining after preincubation with the blocking peptide (unpublished results).

Accordingly, we examined the effect of intracellular application of Syt1 Ab on somatodendritic DA release (Fig. 7*B–D*). Interestingly, D2IC amplitude evoked by phasic stimulation was unaltered by single-cell application of Syt1 Ab in WT SNc DA neurons, with no difference between the initial and final amplitudes over the same recording period during which Syt7 Ab (10 μg/mL) attenuated D2ICs (final: 105 ± 11% of initial, $n = 6$; $p = 0.77$, paired *t* test; compare Figs. 7*B*, 2*A*). However,

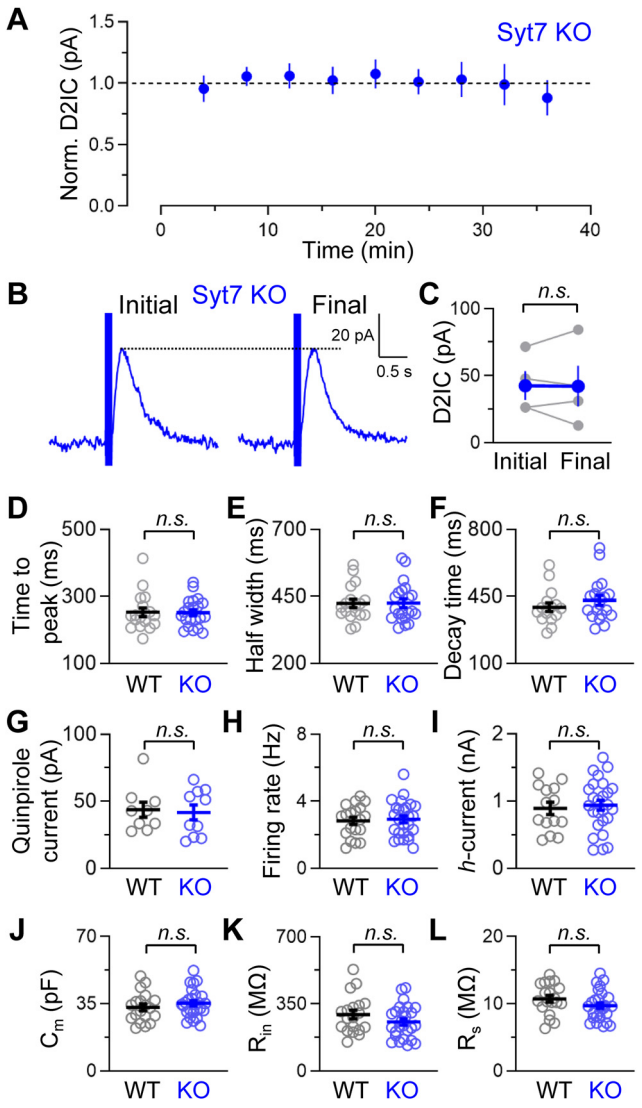

Figure 6. Characteristics of persistent D2ICs in SNc DA neurons from Syt7 KO mice. ***A***, Stability of phasic D2ICs in SNc DA neurons from Syt7 KO mice recorded in 2.4 mM $[Ca^{2+}]_o$. ***B***, Representative D2ICs after establishing whole-cell recording (initial) and at the end of the recording period (final). ***C***, Quantification of D2IC amplitude (final: 93 ± 14% of initial, $n = 4$; $p = 0.95$, unpaired t test). ***D***, Time to peak (WT: 253 ± 13 ms, $n = 18$; KO: 251 ± 9 ms, $n = 21$; $p = 0.93$, unpaired t test). ***E***, Half-width (WT: 424 ± 15 ms, $n = 18$; KO: 425 ± 16 ms, $n = 21$; $p = 0.98$, unpaired t test). ***F***, Decay time constant (WT: 394 ± 21 ms, $n = 16$; KO: 429 ± 24 ms, $n = 19$; $p = 0.32$, unpaired t test). ***G***, Quinpirole-evoked D_2 currents (WT: 43.7 ± 5.3 pA, $n = 9$; Syt7 KO: 41.6 ± 5.2 pA, $n = 10$; $p = 0.79$, paired t test). ***H***, Spontaneous activity (WT: 2.8 ± 0.2 Hz, $n = 19$; Syt7 KO: 2.9 ± 0.2 Hz, $n = 26$; $p = 0.75$, unpaired t test). ***I***, h-current (WT: 0.89 ± 0.09 nA, $n = 14$; Syt7 KO: 0.93 ± 0.07 nA, $n = 26$; $p = 0.72$, unpaired t test). ***J***, Cell capacitance (WT: 33.1 ± 1.7 pF, $n = 19$; Syt7 KO: 35.1 ± 1.4 pF, $n = 26$; $p = 0.35$, unpaired t test). ***K***, Input resistance (WT: 293.9 ± 22.1 MΩ, $n = 19$; Syt7 KO: 255.8 ± 16.5 MΩ, $n = 26$; $p = 0.17$, unpaired t test). ***L***, Series resistance (WT: 8.4 ± 0.8 MΩ, $n = 19$; Syt7 KO: 9.7 ± 0.4 MΩ, $n = 26$; $p = 0.14$, unpaired t test). n.s., Not significant.

intracellular Syt1 Ab led to a significant decrease in D2IC amplitude in SNc DA neurons from Syt7 KO mice (final D2IC amplitude: 63 ± 7% of initial, $n = 5$; $p = 0.0027$, paired t test; Fig. 7*B–D*). In contrast, the initial and final amplitudes of five-pulse evoked D2ICs recorded with Syt1 Ab and its blocking peptide (20 µg/mL) in the pipette did not differ (Syt1 Ab + BP: final, 100 ± 7% of initial, $n = 5$; $p = 0.71$, paired t tests; Fig. 7*B–D*). Quinpirole-induced currents were unaltered by Syt1 Ab in the pipette in Syt7 KO mice, indicating no effect on D2 receptor or GIRK channel function (Fig. 7*C,D*). Moreover, in tested cells filled with Neurobiotin 488 and identified as DAergic by TH immunoreactivity, Syt1 Ab infiltrated the perikaryon and proximal dendrites of recorded SNc DA neurons in both WT (five cells) and Syt7 KO mice (six cells; Fig. 7*E*). Last, to test whether responsiveness to Syt1 Ab in Syt7 KOs might involve the upregulation of Syt1, we quantified Syt1 protein in WT and KO midbrain and striatal tissue ($n = 3$ mice/genotype), and found no difference between the genotypes for either region (Fig. 7*F,G*). Correspondingly, Syt1 immunostaining was indistinguishable between WT and Syt7 KO tissue (not illustrated). Together, these findings indicate that Ca^{2+} sensing for somatodendritic DA release in SNc is achieved primarily, but not exclusively, by Syt7 in WT animals, and that Syt1 can provide functional replacement when Syt7 is absent.

Syt1 function in WT mice

As described above, we found that the amplitudes of one-pulse-evoked D2ICs did not differ between WT and Syt7 KO mice, in either 1.2 or 2.4 mM $[Ca^{2+}]_o$ (Fig. 5*A,B*). These data imply that tonic somatodendritic DA release uses a Ca^{2+} sensor other than Syt7, a role for which Syt1 was again the logical candidate (Fig. 7*A*). To test the influence of Syt1 on tonic somatodendritic DA release, we examined the effect of intracellular application of Syt1 Ab on one-pulse evoked D2IC amplitude in WT SNc DA neurons. Intracellular Syt1 Ab application led to a significant decrease in D2IC amplitude (final: 50 ± 5% of initial, $n = 5$; $p = 0.004$, paired t test; Fig. 7*H–J*). This contrasts with the absence of effect of Syt1 Ab on phasic D2ICs (Fig. 7*B–D*). When Syt1 Ab was applied with its blocking peptide (20 µg/mL), the effect of Syt1 Ab on one-pulse evoked D2ICs was prevented, such that the final D2IC amplitude did not differ from initial over the same recording period (Syt1 Ab + BP: final, 95 ± 2% of initial, $n = 5$; $p = 0.15$, paired t tests; Fig. 7*H–J*). These data demonstrate that Syt1 plays a role in tonic somatodendritic DA release, but not phasic release, thus illustrating that both Syt1 and Syt7 are required for the full repertoire of stimulus-evoked somatodendritic DA release.

Discussion

Our initial goal was to determine whether, and in what way, Syt7 contributes to somatodendritic DA release in SNc DA neurons. We tested this using intracellular application of a validated Syt7 Ab and genetic Syt7 deletion. These approaches have complementary advantages: the use of Syt7 Ab allows assessment of the acute effect of Syt7 impairment in individual SNc DA neurons without affecting neighboring cells (Hikima et al., 2021), whereas global Syt7 KO mice provide unambiguous deletion of Syt7 (Chakrabarti et al., 2003; Jackman et al., 2016).

We found that intracellular Syt7 Ab suppressed phasic D2ICs, without affecting currents induced by external application of a D2 receptor agonist, quinpirole, confirming the inhibition of DA release, rather than altered D2 receptor or GIRK channel function. Intracellular Syt7 Ab also affected the Ca^{2+} dependence of somatodendritic DA release in SNc, with loss of evoked D2ICs in submillimolar $[Ca^{2+}]_o$. A similar change in Ca^{2+} dependence was seen in DA neurons from Syt7 KO mice. These data are consistent with the high affinity of Syt7 for Ca^{2+} (Sugita et al., 2002; Hui et al., 2005) and show that Syt7 underlies the persistence of somatodendritic DA release in submillimolar $[Ca^{2+}]_o$, which has been reported previously (Chen and Rice, 2001; Chen et al., 2011; Mendez et al., 2011). Evidence for a similar role of Syt7 in axonal DA release has also been described (Kissiwaa et al., 2021).

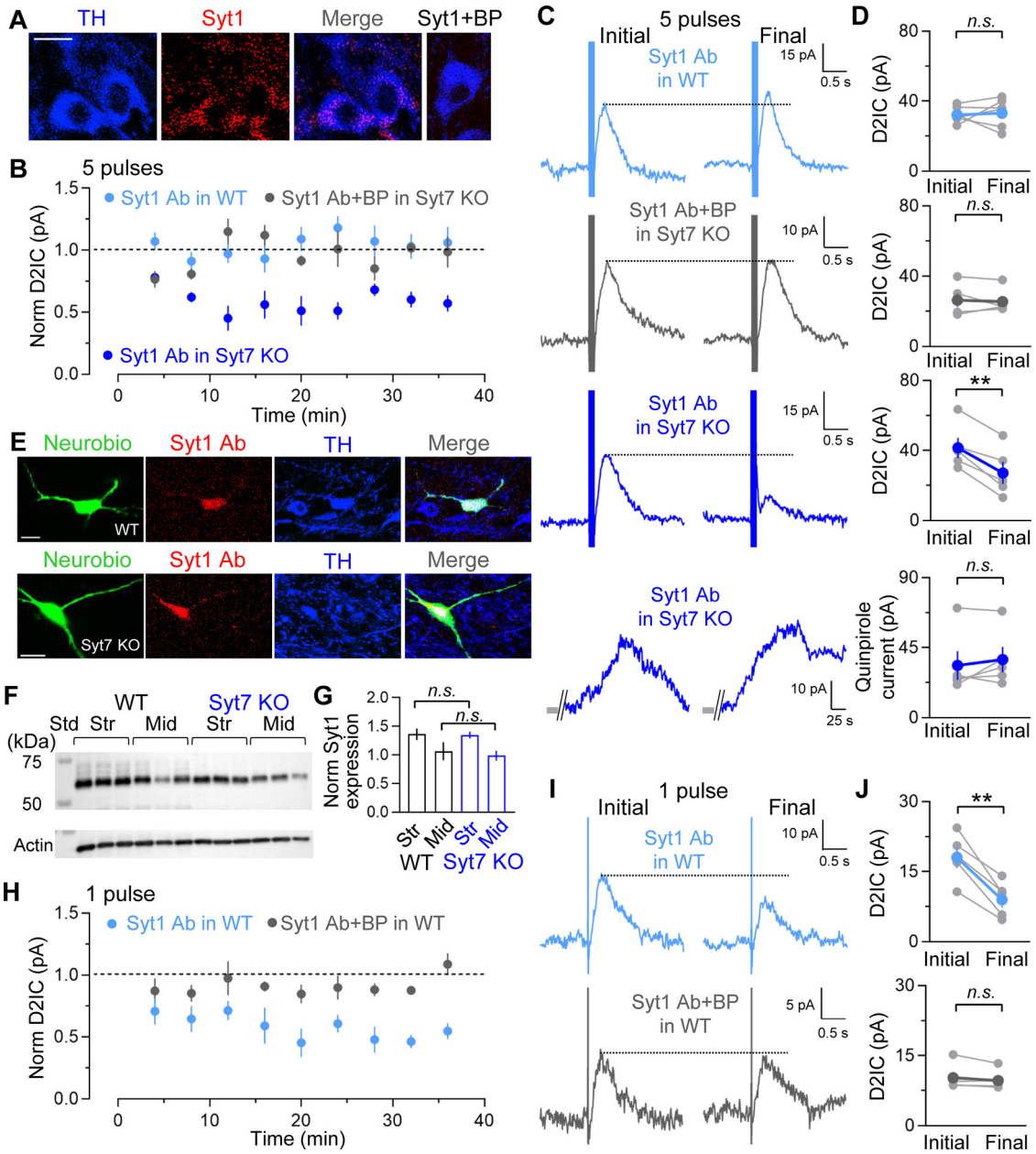

Figure 7. Intracellular application of Syt1 Ab decreases D2IC amplitude in Syt7 KO mice, but not in WT mice. ***A***, Representative images showing immunostaining for Syt1 (red) and TH (blue) in the SNc of a coronal section. Preadsorption of Syt1 with its BP resulted in the loss of Syt1 immunostaining (Syt1+BP). Scale bar, 10 μm. ***B***, Average time course of changes in the amplitude of burst-evoked D2ICs (five pulses, 40 Hz) in 2.4 mM $[Ca^{2+}]_o$ with Syt1 Ab in the recording pipette. Intracellular application of Syt1 Ab deceased amplitude in Syt7 KO mice, but not in WT mice. ***C***, Representative initial and final D2ICs with Syt1 Ab in the pipette in WT (light blue) or Syt7 KO (blue) SNc DA neurons. Below, Representative D2 currents evoked by brief superfusion of quinpirole (250 nM, 15 s) with Syt1 Ab in the pipette. ***D***, Quantification of D2IC amplitude with Syt1 Ab in the pipette (Syt1 Ab in WT: final, 105 ± 11% of initial, $n = 6$, $p = 0.78$; Syt1 Ab+BP in WT: final, 100 ± 7% of initial, $n = 5$, $p = 0.71$; Syt1 Ab in Syt7 KO: final, 63 ± 7% of initial, $n = 5$; paired *t* test). Quantification of quinpirole-evoked D2 currents in the presence of Syt1 Ab (Syt1 Ab: final, 119 ± 15% of initial, $n = 5$; $p = 0.76$, paired *t* test). ***E***, Representative immunostaining of Syt1 Ab and TH in the SNc in a horizontal slice after whole-cell recording. Neurobiotin 488 was used to identify the patch-clamped cell and was introduced with Syt1 Ab via the recording pipette ($n = 6$ slices in three WT mice; $n = 7$ slices in Syt7 KO mice). Scale bar, 10 μm. ***F***, Immunoblots for Syt1 in striatum (Str) and midbrain (Mid) from WT and Syt7 KO mice ($n = 3$ mice/genotype). ***G***, Quantification of Syt1 protein in WT and Syt7 KO midbrain and striatal tissue. ***H***, Average time course of changes in the amplitude of one-pulse evoked D2ICs in 2.4 mM $[Ca^{2+}]_o$ with Syt1 Ab in the recording pipette. Intracellular application of Syt1 Ab decreased amplitude in WT mice, but not with Syt1 Ab+BP. ***I***, Representative initial and final D2ICs in WT SNc DA neurons recorded with Syt1 Ab or with Syt1 Ab+BP in the pipette. ***J***, Quantification of D2IC amplitude with single-cell application of Syt1 Ab or Syt1+BP (Syt1 Ab: final, 50 ± 5% of initial, $n = 5$; Syt1 Ab+BP: final, 95 ± 2% of initial, $n = 5$; $p = 0.15$, paired *t* test). Scale bars: ***A***, ***G***, 20 μm. n.s., Not significant. $^{**}p < 0.01$.

Notably, the loss of phasic-evoked D2ICs in low $[Ca^{2+}]_o$, whether recorded with Syt7 Ab or in DA neurons from Syt7 KO mice, shows the absence of a compensatory mechanism to enable DA release. In millimolar $[Ca^{2+}]_o$, however, robust phasic DA release was seen in Syt7 KOs, implicating an alternative Ca^{2+} sensor under these conditions. We found that Syt1 substituted for Syt7 in phasic DA release after Syt7 deletion and facilitated tonic DA release in WT mice. Overall, our data reveal complementary roles for Syt7 and Syt1 in somatodendritic DA release. By extension, these may contribute to the discrete roles of SNc DA neurons in motor and reward behaviors, in that tonic spiking is linked to self-paced movement whereas burst activity is related

to reward prediction (Niv et al., 2005; Schultz, 2007; da Silva et al., 2018).

Ca^{2+} dependence of somatodendritic DA release in the SNc

Members of the Syt family provide Ca^{2+} sensing for exocytosis (Brose et al., 1992; Südhof, 2002). Previous studies in cultured DA neurons showed that the downregulation of Syt7 prevents K^+-evoked DA release in low $[Ca^{2+}]_o$, whereas the downregulation of Syt1 has no effect (Mendez et al., 2011). Here, we found that the evoked somatodendritic DA release seen in low $[Ca^{2+}]_o$ is absent when recorded with Syt7 Ab in the pipette or after Syt7 deletion. Hill plots showed an increase in the $[Ca^{2+}]_o$ EC_{50} for DA release with single-cell Syt7 Ab application and in Syt7 KOs, confirming that Syt7 governs the sensitivity of somatodendritic DA release to low $[Ca^{2+}]_o$. Although the EC_{50} for Ca^{2+} in WT mice was somewhat higher than in our previous Ca^{2+} dependence study using FSCV in guinea pig slices (Chen et al., 2011), the prior experiments included a DA uptake inhibitor that would facilitate DA detection at lower $[Ca^{2+}]_o$ than in the present work.

Analysis of single-cell Ca^{2+} dependence data for DA release from WT SNc neurons gave a Hill coefficient of 1.8, which is similar to that reported previously (Chen et al., 2011). The usual Hill coefficient for Ca^{2+} in synaptic transmission is 2.5–5 (Augustine et al., 1985; Sun et al., 2007; Chen et al., 2011), indicating that the Ca^{2+} cooperativity required for somatodendritic DA release is lower than that for classical fast synaptic transmission. In SNc, low cooperativity appears to be mediated by Syt7, in that Syt7 Ab or Syt7 deletion increased the Hill coefficients for somatodendritic DA release to 3.3 with Syt7 Ab and to 2.6 in Syt7 KOs.

Facilitation of phasic somatodendritic DA release by Syt7

We found that D2ICs evoked by phasic stimulation in SNc DA neurons lacking Syt7 were more sensitive to a change in $[Ca^{2+}]_o$ in the physiological range than those from WT mice (Figs. 4, 5). In contrast, the absence of Syt7 had no effect on the sensitivity of one-pulse evoked D2ICs to changes in millimolar $[Ca^{2+}]_o$. These data imply a greater role for Syt7 in phasic versus tonic somatodendritic DA release. The influence of Syt7 on phasic DA release can be understood by considering that the DA release response is detected after the end of a stimulus train (Fig. 5*A*), at a time when phasic stimulated $[Ca^{2+}]_i$ is still elevated, but falling (Hage and Khaliq, 2015). Our data suggest that high-Ca^{2+} affinity Syt7 mediates release during this poststimulus phase, a facilitation that is lost in Syt7 KOs. Studies in other neuron types have shown that Syt7 responds to residual $[Ca^{2+}]_i$ to facilitate asynchronous transmitter release (Bacaj et al., 2013; Kaeser and Regehr, 2014; Luo et al., 2015; Jackman et al., 2016; Chen et al., 2017; Jackman and Regehr, 2017; Luo and Südhof, 2017; Turecek and Regehr, 2018). The slow rate of Ca^{2+} dissociation after binding to Syt7 (Brandt et al., 2012) would prolong the release process further. Thus, the greater influence of Syt7 on phasic versus tonic DA release leads to an increase in the contrast between phasic and tonic release, which would amplify feedback inhibition of DA neuron activity after a burst of action potentials, including those associated with motor acceleration and reward prediction (Schultz, 2007; Howe and Dombeck, 2016; da Silva et al., 2018). Facilitation of phasic DA release in SNc by Syt7 is supported by evidence in a recent preprint (Kissiwaa et al., 2021).

Functional substitution of Syt1 for Syt7

The persistence of phasic D2ICs in Syt7 KO mice in millimolar $[Ca^{2+}]_o$ points to the involvement of additional Ca^{2+} sensors. Prior work indicates that midbrain DA neurons express four Syt isoforms (1, 4, 7, and 11; Glavan and Zivin, 2005; Mendez et al., 2011; Delignat-Lavaud et al., 2022), of which Syt1 and Syt7 contain the Ca^{2+}-binding domains required to activate the SNARE complex and initiate transmitter release (Südhof, 2002). Here, we identified Syt1 protein in SNc DA neurons by immunostaining. However, we found no role for Syt1 in phasic somatodendritic DA release in WT neurons, indicated by the lack of effect of intracellular Syt1 Ab on D2IC amplitude. In contrast, intracellular Syt1 Ab in DA neurons from Syt7 KO mice markedly decreased the amplitude of pulse train-evoked D2ICs, showing that Syt1 can mediate release in the absence of Syt7. This substitution of function is contingent on a sufficiently high $[Ca^{2+}]_o$, which is consistent with the low Ca^{2+} sensitivity of Syt1. Moreover, the increases in the Hill coefficient that we found when Syt7 was absent or inhibited by Syt7 Ab are consistent with the high-cooperativity of Syt1 (Sugita et al., 2002; Hui et al., 2005). The possibility that Syt7 deletion might result in the upregulation of Syt1 expression was negated by our finding that immunoblots from midbrain and striatum showed no difference in Syt1 levels between WT and Syt7 KO mice.

Our data show that Syt1 can compensate for some, but not all, aspects of Syt7 function. Conversely, previous reports indicate that Syt7 does not substitute well for Syt1. For example, Syt7 does not rescue fast neurotransmission in Syt1-deleted neurons (Xu et al., 2007). Moreover, the deletion of Syt1 in adrenal chromaffin cells leads to the loss of a fast release phase, leaving intact a slow release phase that is lost when Syt7 also is deleted (Schonn et al., 2008). Other Syts may play a role as well; for example, recent evidence indicates functional compensation by Syt4 in VTA DA neurons when Syt7 is deleted (Delignat-Lavaud et al., 2022). Overall, in DA neurons, the high affinity of Syt7 for Ca^{2+} coupled with a slow dissociation constant (Brandt et al., 2012) is well matched to the relatively slow kinetics of G-protein-activated DA receptors.

Involvement of Syt1 in tonic somatodendritic DA release

Although we found that single-cell application of Syt1 Ab in WT SNc DA neurons did not alter somatodendritic DA release evoked by pulse trains, Syt1 Ab decreased D2ICs evoked by one-pulse stimulation. These data imply a role for Syt1 in tonic, but not in phasic, somatodendritic DA release. In typical fast synapses, synchronous release is triggered by low-affinity Ca^{2+} sensors Syt1, Syt2, or Syt9 (Geppert et al., 1994; Xu et al., 2007). The rapid Ca^{2+} influx following an action potential transiently increases intracellular Ca^{2+} concentration ($[Ca^{2+}]_i$) to a level sufficient to activate Syt1 and trigger vesicular release (Jackman and Regehr, 2017; Volynski and Krishnakumar, 2018). The demonstrated role of Syt1 in one-pulse evoked DA release implies Ca^{2+} influx sufficient to activate Syt1. In contrast, the similarity of one-pulse evoked D2ICs between WT and Syt7 KOs implies a limited role for Syt7 in tonic release. This is consistent with the absence of effect of Syt7 deletion on one-pulse evoked inhibitory postsynaptic currents in cortical neurons (Maximov et al., 2008) and, again, highlights the established role of Syt7 in asynchronous release. Thus, Syt1 and Syt7 operate as Ca^{2+} sensors subserving distinct patterns of somatodendritic DA release.

Conclusions

We have shown that Syt7 plays a predominant role in phasic somatodendritic DA release, with substitution by Syt1 when Syt7 is absent, and that Syt1 plays a predominant role in tonic somatodendritic DA release. Intriguingly, Syt7 has been identified as a

candidate risk factor for behavioral abnormalities in bipolar disorder and cognitive impairment in Alzheimer's disease (Barthet et al., 2018; Shen et al., 2020; Xie et al., 2021), whereas Syt1 has been associated with neurologic deficits, including movement and neurodevelopmental disorders (Baker et al., 2015, 2018). These effects could reflect in part altered DA neuron regulation through the roles of Syt7 and Syt1 identified here, extending the potential importance of the findings.

References

Augustine GJ, Charlton MP, Smith SJ (1985) Calcium entry and transmitter release at voltage-clamped nerve terminals of squid. J Physiol 367:163–181.

Bacaj T, Wu D, Yang X, Morishita W, Zhou P, Xu W, Malenka RC, Südhof TC (2013) Synaptotagmin-1 and -7 trigger synchronous and asynchronous phases of neurotransmitter release. Neuron 80:947–959.

Baker K, Gordon SL, Grozeva D, van Kogelenberg M, Roberts NY, Pike M, Blair E, Hurles ME, Chong WK, Baldeweg T, Kurian MA, Boyd SG, Cousin MA, Raymond FL (2015) Identification of a human synaptotagmin-1 mutation that perturbs synaptic vesicle cycling. J Clin Invest 125:1670–1678.

Baker K, et al. (2018) SYT1-associated neurodevelopmental disorder: a case series. Brain 141:2576–2591.

Banerjee A, Lee J, Nemcova P, Liu C, Kaeser PS (2020) Synaptotagmin-1 is the Ca^{2+} sensor for fast striatal dopamine release. Elife 9:e58359.

Barthet G, Jordà-Siquier T, Rumi-Masante J, Bernadou F, Müller U, Mulle C (2018) Presenilin-mediated cleavage of APP regulates synaptotagmin-7 and presynaptic plasticity. Nat Commun 9:4780.

Beckstead MJ, Grandy DK, Wickman K, Williams JT (2004) Vesicular dopamine release elicits an inhibitory postsynaptic current in midbrain dopamine neurons. Neuron 42:939–946.

Beckstead MJ, Ford CP, Phillips PEM, Williams JT (2007) Presynaptic regulation of dendrodendritic dopamine transmission. Eur J Neurosci 26:1479–1488.

Bergquist F, Niazi HS, Nissbrandt H (2002) Evidence for different exocytosis pathways in dendritic and terminal dopamine release in vivo. Brain Res 950:245–253.

Brandt DS, Coffman MD, Falke JJ, Knight JD (2012) Hydrophobic contributions to the membrane docking of synaptotagmin 7 C2A domain: mechanistic contrast between isoforms 1 and 7. Biochemistry 51:7654–7664.

Brose N, Petrenko AG, Südhof TC, Jahn R (1992) Synaptotagmin: a calcium sensor on the synaptic vesicle surface. Science 256:1021–1025.

Chakrabarti S, Kobayashi KS, Flavell RA, Marks CB, Miyake K, Liston DR, Fowler KT, Gorelick FS, Andrews NW (2003) Impaired membrane resealing and autoimmune myositis in synaptotagmin VII–deficient mice. J Cell Biol 162:543–549.

Chen B, Patel JC, Moran KA, Rice ME (2011) Differential calcium dependence of axonal versus somatodendritic dopamine release, with characteristics of both in the ventral tegmental area. Front Syst Neurosci 5:39.

Chen BT, Rice ME (2001) Novel Ca^{2+} dependence and time course of somatodendritic dopamine release: substantia nigra versus striatum. J Neurosci 21:7841–7847.

Chen C, Satterfield R, Young SM, Jonas P (2017) Triple function of synaptotagmin 7 ensures efficiency of high-frequency transmission at central GABAergic synapses. Cell Rep 21:2082–2089.

Courtney NA, Mamaligas AA, Ford CP (2012) Species differences in somatodendritic dopamine transmission determine D_2-autoreceptor-mediated inhibition of ventral tegmental area neuron firing. J Neurosci 32:13520–13528.

da Silva JA, Tecuapetla F, Paixão V, Costa RM (2018) Dopamine neuron activity before action initiation gates and invigorates future movements. Nature 554:244–248.

Delignat-Lavaud B, Kano B, Ducrot C, Massé I, Mukherjee S, Giguère N, Moquin L, Lévesque C, Nanni SB, Bourque M-J, Rosa-Neto P, Lévesque D, De Beaumont L, Trudeau L-E (2021) The calcium sensor synaptotagmin-1 is critical for phasic axonal dopamine release in the striatum and mesencephalon, but is dispensable for basic motor behaviors in mice. bioRxiv. doi: 10.1101/2021.09.15.460511.

Delignat-Lavaud B, Ducrot C, Kouwenhoven W, Feller N, Trudeau LÉ (2022) Implication of synaptotagmins 4 and 7 in activity-dependent somatodendritic dopamine release in the ventral midbrain. Open Biol 12:210339.

Ford CP, Mark GP, Williams JT (2006) Properties and opioid inhibition of mesolimbic dopamine neurons vary according to target location. J Neurosci 26:2788–2797.

Ford CP, Gantz SC, Phillips PEM, Williams JT (2010) Control of extracellular dopamine at dendrite and axon terminals. J Neurosci 30:6975–6983.

Fortin GD, Desrosiers CC, Yamaguchi N, Trudeau L-É (2006) Basal somatodendritic dopamine release requires SNARE proteins. J Neurochem 96:1740–1749.

Gantz SC, Bunzow JR, Williams JT (2013) Spontaneous inhibitory synaptic currents mediated by a G protein-coupled receptor. Neuron 78:807–812.

Geffen LB, Jessell TM, Cuello AC, Iversen LL (1976) Release of dopamine from dendrites in rat substantia nigra. Nature 260:258–260.

Geppert M, Goda Y, Hammer RE, Li C, Rosahl TW, Stevens CF, Südhof TC (1994) Synaptotagmin I: a major Ca^{2+} sensor for transmitter release at a central synapse. Cell 79:717–727.

Glavan G, Zivin M (2005) Differential expression of striatal synaptotagmin mRNA isoforms in hemiparkinsonian rats. Neuroscience 135:545–554.

Grace A, Bunney B (1984) The control of firing pattern in nigral dopamine neurons: burst firing. J Neurosci 4:2877–2890.

Gustavsson N, Wei S-H, Hoang DN, Lao Y, Zhang Q, Radda GK, Rorsman P, Südhof TC, Han W (2009) Synaptotagmin-7 is a principal Ca^{2+} sensor for Ca^{2+}-induced glucagon exocytosis in pancreas. J Physiol 587:1169–1178.

Hage TA, Khaliq ZM (2015) Tonic firing rate controls dendritic Ca^{2+} signaling and synaptic gain in substantia nigra dopamine neurons. J Neurosci 35:5823–5836.

Hikima T, Lee CR, Witkovsky P, Chesler J, Ichtchenko K, Rice ME (2021) Activity-dependent somatodendritic dopamine release in the substantia nigra autoinhibits the releasing neuron. Cell Rep 35:108951.

Howe MW, Dombeck DA (2016) Rapid signalling in distinct dopaminergic axons during locomotion and reward. Nature 535:505–510.

Hui E, Bai J, Wang P, Sugimori M, Llinas RR, Chapman ER (2005) Three distinct kinetic groupings of the synaptotagmin family: candidate sensors for rapid and delayed exocytosis. Proc Natl Acad Sci USA 102:5210–5214.

Jackman SL, Regehr WG (2017) The mechanisms and functions of synaptic facilitation. Neuron 94:447–464.

Jackman SL, Turecek J, Belinsky JE, Regehr WG (2016) The calcium sensor synaptotagmin 7 is required for synaptic facilitation. Nature 529:88–91.

Jaffe EH, Marty A, Schulte A, Chow RH (1998) Extrasynaptic vesicular transmitter release from the somata of substantia nigra neurons in rat midbrain slices. J Neurosci 18:3548–3553.

Kaeser PS, Regehr WG (2014) Molecular mechanisms for synchronous, asynchronous, and spontaneous neurotransmitter release. Annu Rev Physiol 76:333–363.

Kissiwaa SA, Lebowitz JJ, Engeln KA, Bowman AM, Williams JT, Jackman SL (2021) Synaptotagmin-7 enhances phasic dopamine release. bioRxiv 464710.

Lacey MG, Mercuri NB, North RA (1988) On the potassium conductance increase activated by GABAB and dopamine D2 receptors in rat substantia nigra neurones. J Physiol 401:437–453.

Lee CR, Machold RP, Witkovsky P, Rice ME (2013) TRPM2 channels are required for NMDA-induced burst firing and contribute to H_2O_2-dependent modulation in substantia nigra pars reticulata GABAergic neurons. J Neurosci 33:1157–1168.

Luo F, Südhof TC (2017) Synaptotagmin-7-mediated asynchronous release boosts high-fidelity synchronous transmission at a central synapse. Neuron 94:826–839.e3.

Luo F, Bacaj T, Südhof TC (2015) Synaptotagmin-7 is essential for Ca^{2+}-triggered delayed asynchronous release but not for Ca^{2+}-dependent vesicle priming in retinal ribbon synapses. J Neurosci 35:11024–11033.

Maximov A, Lao Y, Li H, Chen X, Rizo J, Sørensen JB, Südhof TC (2008) Genetic analysis of synaptotagmin-7 function in synaptic vesicle exocytosis. Proc Natl Acad Sci USA 105:3986–3991.

Mendez JA, Bourque M-J, Fasano C, Kortleven C, Trudeau L-E (2011) Somatodendritic dopamine release requires synaptotagmin 4 and 7 and the participation of voltage-gated calcium channels. J Biol Chem 286:23928–23937.

Niv Y, Daw ND, Dayan P (2005) How fast to work: response vigor, motivation and tonic dopamine. Adv Neural Inf Process Syst 18:1019–1026.

Patel JC, Witkovsky P, Avshalumov MV, Rice ME (2009) Mobilization of calcium from intracellular stores facilitates somatodendritic dopamine release. J Neurosci 29:6568–6579.

Pinheiro PS, Houy S, Sørensen JB (2016) C2-domain containing calcium sensors in neuroendocrine secretion. J Neurochem 139:943–958.

Rice ME, Richards CD, Nedergaard S, Hounsgaard J, Nicholson C, Greenfield SA (1994) Direct monitoring of dopamine and 5-HT release in substantia nigra and ventral tegmental area in vitro. Exp Brain Res 100:395–406.

Rice ME, Cragg SJ, Greenfield SA (1997) Characteristics of electrically evoked somatodendritic dopamine release in substantia nigra and ventral tegmental area in vitro. J Neurophysiol 77:853–862.

Robinson BG, Bunzow JR, Grimm JB, Lavis LD, Dudman JT, Brown J, Neve KA, Williams JT (2017) Desensitized D2 autoreceptors are resistant to trafficking. Sci Rep 7:4379.

Robinson BG, Cai X, Wang J, Bunzow JR, Williams JT, Kaeser PS (2019) RIM is essential for stimulated but not spontaneous somatodendritic dopamine release in the midbrain. Elife 8:e47972.

Sathler MF, Khatri L, Roberts JP, Schmidt IG, Zaytseva A, Kubrusly RCC, Ziff EB, Kim S (2021) Phosphorylation of the AMPA receptor subunit GluA1 regulates clathrin-mediated receptor internalization. J Cell Sci 134:jcs257972.

Schneggenburger R, Neher E (2000) Intracellular calcium dependence of transmitter release rates at a fast central synapse. Nature 406:889–893.

Schonn J-S, Maximov A, Lao Y, Südhof TC, Sørensen JB (2008) Synaptotagmin-1 and -7 are functionally overlapping Ca^{2+} sensors for exocytosis in adrenal chromaffin cells. Proc Natl Acad Sci USA 105:3998–4003.

Shen W, Wang Q-W, Liu Y-N, Marchetto MC, Linker S, Lu S-Y, Chen Y, Liu C, Guo C, Xing Z, Shi W, Kelsoe JR, Alda M, Wang H, Zhong Y, Sui S-F, Zhao M, Yang Y, Mi S, Cao L, et al (2020) Synaptotagmin-7 is a key factor for bipolar-like behavioral abnormalities in mice. Proc Natl Acad Sci USA 117:4392–4399.

Schultz W (2007) Multiple dopamine functions at different time courses. Annu Rev Neurosci 30:259–288.

Südhof TC (2002) Synaptotagmins: why so many? J Biol Chem 277:7629–7632.

Südhof TC, Rizo J (1996) Synaptotagmins: C_2-domain proteins that regulate membrane traffic. Neuron 17:379–388.

Sugita S, Han W, Butz S, Liu X, Fernández-Chacón R, Lao Y, Südhof TC (2001) Synaptotagmin VII as a plasma membrane Ca^{2+} sensor in exocytosis. Neuron 30:459–473.

Sugita S, Shin OH, Han W, Lao Y, Südhof TC (2002) Synaptotagmins form a hierarchy of exocytotic Ca^{2+} sensors with distinct Ca^{2+} affinities. EMBO J 21:270–280.

Sun J, Pang ZP, Qin D, Fahim AT, Adachi R, Südhof TC (2007) A dual-Ca^{2+}-sensor model for neurotransmitter release in a central synapse. Nature 450:676–682.

Turecek J, Regehr WG (2018) Synaptotagmin 7 mediates both facilitation and asynchronous release at granule cell synapses. J Neurosci 38:3240–3251.

Volynski KE, Krishnakumar SS (2018) Synergistic control of neurotransmitter release by different members of the synaptotagmin family. Curr Opin Neurobiol 51:154–162.

Witkovsky P, Patel JC, Lee CR, Rice ME (2009) Immunocytochemical identification of proteins involved in dopamine release from the somatodendritic compartment of nigral dopaminergic neurons. Neuroscience 164:488–496.

Xie Y, Zhi K, Meng X (2021) Effects and mechanisms of synaptotagmin-7 in the hippocampus on cognitive impairment in aging mice. Mol Neurobiol 58:5756–5771.

Xu J, Mashimo T, Südhof TC (2007) Synaptotagmin-1, -2, and -9: Ca^{2+} sensors for fast release that specify distinct presynaptic properties in subsets of neurons. Neuron 54:567–581.